ViewRay™ References

The field of MRI-guided radiation therapy draws on the research of dedicated radiation oncologists, physicists, and other scientists who have studied various aspects of medical imaging, treatment planning, radiation therapy delivery, and tumor and organ motion. These references represent a sampling of the significant work these researchers have contributed to the advancement of MRI-guided radiation therapy.

1) Dempsey, J., Romeijn, H., Palta, J., Mutic, S., Low, D., Li, J., et al. (2005). A Device For Realtime 3D Image-Guided IMRT. *International Journal of Radiation OncologyBiologyPhysics*, 63, S202-S202.

2) Dempsey, J., Romeijn, H., Palta, J., Mutic, S., Low, D., Li, J., et al. (2006). WE-E-ValA-06: A Real-Time MRI Guided External Beam Radiotherapy Delivery System. *Medical Physics*, 33(6), 2254.

3) Fox, C., Aleman, D., Romeijn, H., Li, J., & Dempsey, J. (2006). 2825Gamma-Ray Intensity Modulated Radiation Therapy. *International Journal of Radiation OncologyBiologyPhysics*, 66(3), S673-S674.

4) Green, O., Goddu, S., & Mutic, S. (2012). SU-E-T-352: Commissioning and Quality Assurance of the First Commercial Hybrid MRI-IMRT System. *Medical Physics*, 39(6), 3785.

5) Green, O., Hu, Y., Noel, C., Olsen, J. & Mutic, S. (2012). Observation of Radiation-induced Tissue Signal Intensity Changes With the First Commercial MRI-guided IMRT System. *International Journal of Radiation OncologyBiologyPhysics*, 84, S758-759.

6) Green, O., Hu, Y., Zeng, Q., Nana, R., Patrick, J., Shvartsman, S., Eagan, T., Mutic, S., & Dempsey, J. (2012). Realizing the QUANTEC Vision by Applying Weighted Hybrid Iterative Spiral K-Space Encoding Estimation (WHISKEE) to Actual Dose (D_A) Accumulation via Image Deformation (D_AA_VID). *International Journal of Radiation OncologyBiologyPhysics*, 84, S758-759.

7) Green, O., Wooten, H., Hu, Y., Santanam, L., Li, H. & Mutic, S. (2013). SU-ET-139: Evaluation of Surface, Peripheral, and Buildup Dose in MR-IGRT. *Medical Physics*, 40(6), 236.

8) Goddu, S., Green, O., & Mutic, S. (2012). WE-G-BRB-08: TG-51 Calibration of First Commercial MRI-Guided IMRT System in the Presence of 0.35 Tesla Magnetic Field. *Medical Physics*, 39(6), 3968.

9) Hsi, W., Vargas, C., Saito, A., Dempsey, J., Keole, S., Lin, L., et al. (2008). Automatic Deformable Registration On Prostate Cine-MRI Images For Studying Intra-fraction Motion In Supine And Prone Position With And Without Rectal Balloon. *International Journal of Radiation OncologyBiologyPhysics*, 72(1), S557-S557.

10) Hu, Y., Green, O., Feng, Y., Du, D., Wooten, O., Li, H. , Santanam, L., Parikh, P., Olsen, J., & Mutic, S. (2013). Image Performance Characterization of an MRI-Guided Radiation Therapy System. *International Journal of Radiation OncologyBiologyPhysics*, 87, S13.

11) Hu, Y., Green, O., Parikh, P., Olsen, J., & Mutic, S. (2012). TH-E-BRA-07: Initial Experience with the ViewRay System-Quality Assurance Testing of the Imaging Component. *Medical Physics,* 39(6), 4013.

12) Jaffray, D., Mutic, S., Fallone, B., & Raaymakers, B. (2013). MO-A-WAB-01: MRI-Guided Radiation Therapy. *Medical Physics*, 40(6), 390.

13) Mutic S. (2012). WE-A-BRA-02: First Commercial Hybrid MRI-IMRT System. *Medical Physics*, 39(6), 3934.

14) Noel, C., Olsen, J., Green, O., Hu, Y. & Parikh, P. (2012). TU-G-217A-09: Feasibility of Bowel Tracking Using Onboard Cine MRI for Gated Radiotherapy. *Medical Physics*, 39(6), 3928.

15) Olsen, J., Noel, C., Spencer, C., Green, O., Hu, Y., Mutic, S., & Parikh, P. (2012). Feasibility of Single and Multiplane Cine MR for Monitoring Tumor Volumes and Organs-at-Risk (OARs) Position During Radiation Therapy. *International Journal of Radiation OncologyBiologyPhysics*, 84, S742.

16) Parikh, P., Noel, C., Spencer, C., Green, O., Hu, Y., Mutic, S., & Olsen, J. (2012). Comparison of Onboard Low-field MRI Versus CBCT/MVCT for Anatomy Identification in Radiation Therapy. *International Journal of Radiation OncologyBiologyPhysics*, 84, S133.

17) Saenz, D., Bayouth J., & Paliwal B. (2013). SU-E-T-614: A Comparison of IMRT Plans for the ViewRay MR-Guided RT System with TomoTherapy and Pinnacle. *Medical Physics*, 40(6), 347.

18) Saito, A., Li, J., Liu, C., Olivier, K., & Dempsey, J. (2006). 2831Accurate Heterogeneous Dose Calculation For Lung Cancer Patients Without High Resolution CT Densities. *International Journal of Radiation OncologyBiologyPhysics*, 66(3), S677-S678.

19) Yanez, R., & Dempsey, J. F. (2007). WE-C-AUD-04: Monte Carlo Simulations Of Air Cavities In Phantoms Submerged In Magnetic Fields. *Medical Physics*, 34(6), 2590.

VIEWRAY | Visibly Different

A Device for Realtime 3D Image-Guided IMRT

Dempsey, J., Romeijn, H., Palta, J., Mutic, S., Low, D., Li, J., et al. (2005). A Device For Realtime 3D Image-Guided IMRT. *International Journal of Radiation OncologyBiologyPhysics*, 63, S202-S202.

http://www.researchgate.net/publication/238227760_A_Device_for_Realtime_3D_Image-Guided_IMRT

ABSTRACT

The authors report the first magnetic resonance (MR) images produced by their prototype MR system integrated with a radiation therapy source. The prototype consists of a 6 MV linac mounted onto the open end of a biplanar 0.2 T permanent MR system which has 27.9 cm pole-to-pole opening with flat gradients (40 mT/m) running under a TMX NRC console. The distance from the magnet isocenter to the linac target is 80 cm. The authors' design has resolved the mutual interferences between the two devices such that the MR magnetic field does not interfere with the trajectory of the electron in the linac waveguide, and the radiofrequency (RF) signals from each system do not interfere with the operation of the other system. Magnetic and RF shielding calculations were performed and confirmed with appropriate measurements. The prototype is currently on a fixed gantry; however, in the very near future, the linac and MR magnet will rotate in unison such that the linac is always aimed through the opening in the biplanar magnet. MR imaging was found to be fully operational during linac irradiation and proven by imaging a phantom with conventional gradient echo sequences. Except for small changes in SNR, MR images produced during irradiation were visually and quantitatively very similar to those taken with the linac turned off. This prototype system provides proof of concept that the design has decreased the mutual interferences sufficiently to allow the development of real-time MR-guided radiotherapy. Low field-strength systems (0.2-0.5 T) have been used clinically as diagnostic tools. The task of the linac-MR system is, however, to provide MR guidance to the radiotherapy beam. Therefore, the 0.2 T field strength would provide adequate image quality for this purpose and, with the addition of fast imaging techniques, has the potential to provide 4D soft-tissue visualization not presently available in image-guided radiotherapy systems. The authors' initial design incorporates a permanent magnet; however, other types of magnets and field strengths could also be incorporated. Usable MR images were obtained during linac irradiation from the linac-MR prototype. The authors' prototype design can be used as the functional starting point in developing real-time MR guidance offering soft-tissue contrast that can be coupled with tumor tracking for real-time adaptive radiotherapy.

A Real-Time MRI Guided External Beam Radiotherapy Delivery System

Dempsey, J., Romeijn, H., Palta, J., Mutic, S., Low, D., Li, J., et al. (2006). WE-E-ValA-06: A Real-Time MRI Guided External Beam Radiotherapy Delivery System. *Medical Physics*, 33(6), 2254.

http://dx.doi.org/10.1118/1.2241803

ABSTRACT

Purpose

We present feasibility studies in support of a real-time MRI guided external beam radiotherapy delivery system currently under commercial development.

Method and Materials

The system, (ViewRay Inc., Renaissance™), combines a low field open MRI scanner and a multi-headed 60Co y-ray IMRT unit equipped with multi-leaf collimators. It is designed so that the center of the field of view of the MRI and the isocenter of the radiotherapy unit coincide. The inherent compatibility of the units allows for the acquisition of fast ciné MRI simultaneous to radiotherapy delivery to assess intra-fraction organ motion. Computational feasibility studies were performed to investigate: the compatibility of the MRI and the 60Co y-ray IMRT unit; the impact of the MRI magnetic field on the dosimetry; and the feasibility of performing accurate heterogeneity dose computations with MRI data.

Results

The 60Co y-ray IMRT unit was found not to significantly impact the operation of the MRI; the y-ray IMRT unit is capable of producing high quality IMRT treatment plans; the MRI magnetic field eliminates contamination electrons and does not significantly perturb the dose distribution in lung, soft tissue, and bone; and accurate heterogeneity dose computations are possible employing only MRI data.

Conclusion

Performing IMRT allows for the seamless integration with, and simultaneous operation of, an open MRI unit. Conflict of Interest: Research sponsored by ViewRay, Inc., Gainesville, Florida USA.

Gamma-Ray Intensity Modulated Radiation Therapy

Fox, C., Aleman, D., Romeijn, H., Li, J., & Dempsey, J. (2006). 2825Gamma-Ray Intensity Modulated Radiation Therapy. *International Journal of Radiation OncologyBiologyPhysics*, 66(3), S673-S674.

http://www.redjournal.org/article/S0360-3016(06)02480-1/fulltext

Article Outline

- Purpose/Objective(s)
- Materials/Methods
- Results
- Conclusions
- Copyright

Purpose/Objective(s)

We compare the quality of gamma-ray based intensity modulated radiation therapy (IMRT) produced using a commercially available Cobalt-60 source and a doubly focused multileaf collimator to linear-accelerator based IMRT. Gamma-ray IMRT is compatible with on-board magnetic resonance imaging (MRI) for real-time image guided radiation therapy (IGRT) and this study was performed evaluate the quality of gamma-ray IMRT for IGRT.

Materials/Methods

The University of Florida optimized radiation therapy (UFORT) in-house treatment-planning system was commissioned with measured data from Cobalt-60, 6MV, and 18MV beamlets. A total of 25 IMRT cases were studied, including 5 H & N, 5 prostate, 5 lung, and 5 breast, and 5 CNS. Treatment plans using a Cobalt-60 gamma-ray based source were compared with 6MV and 18MV linear-accelerator plans. The IMRT treatment plans were optimized with a convex optimization model that can be solved to optimality without the possibility of trapping in local minima. Plans were generated for all cases with 5, 7, 9, 11, 17, 35 and 71 equispaced cone beams. Helical tomotherapy plans with a pitch of 0.5 were also investigated for the 5 H & N cases. Dose volume histograms (DVH) were used to assess the plan quality using standard clinical dose volume constraints.

Results

The same target coverage could be achieved for plans with 5 through 71 beams for all cases. Small variations between the three beam qualities were observed when evaluating plans with standard clinical dose volume constraints on critical structures for all cases studied. Dose to unspecified tissue in the range of 5 to 40 Gy was always lower by 2–7% volume for more penetrating linac beams. Improvements in organ sparing with increasing equidistant beam number were observed for increasing beam number up to 11 beams but yielded marginal improvements for more than 11 beams. Improved tissue sparing at low doses was always observed for prostate cases with increased beam number; however, standard dose volume constraints for targets and critical structures were well below tolerance for all investigated beam numbers.

Conclusions

Gamma-ray IMRT produces high quality IMRT treatment plans for integration with on-board real-time MRI. Beam quality and beam number did not have a significant impact on treatment plan quality as assessed by standard clinical dose volume constraints.

Commissioning and Quality Assurance of the First Commercial Hybrid MRI-IMRT System

Green, O., Goddu, S., & Mutic, S. (2012). SU-E-T-352: Commissioning and Quality Assurance of the First Commercial Hybrid MRI-IMRT System. *Medical Physics*, 39(6), 3785.

http://dx.doi.org/10.1118/1.4735439

Purpose

To describe the commissioning process for the first installed commercial MRI-guided IMRT system (ViewRay, Village of Oakwood, OH) and outline quality assurance methods for this novel treatment modality.

Methods

The ViewRay™ System (510(k) pending) consists of a 0.35-T double-doughnut MRI coupled with a gantry that houses three Co-60 sources,each with an activity up to 15,000 Ci (120° apart). IMRT delivery is enabled by doubly-focused MLCs that serve as the only beam-shaping collimators for each head, allowing a maximum field size of 27.3 cm2 at the 105-cm isocenter. MRIimaging is used prior to and during delivery for setup evaluation, adaptive radiotherapy, and gating. The challenges in commissioning as well as periodic and patient-specific QA arise due to the presence of the magnetic field, unique geometry of this device which is not compatible with many of conventional RT QA devices and techniques, and the penumbra of a 2-cm wide Co-60 source. The following devices were used for commissioning and quality assurance tests: radiochromic and radiographic film, ionization chambers (Exradin A12 & A16), Sun Nuclear's IC Profiler (Melbourne, FL), and a water tank. Tests were conducted to evaluate the beam profiles, penumbra, and PDDs. Also, tests to check MLC accuracy and reproducibility were evaluated.

Results

Tests were developed to validate geometric performance of the device including a comprehensive set of MLC tests. Due to the low strength of the magnetic field, the mean free path of electrons in the ionization chamber volume is too long to have a noticeable curvature; therefore the magnetic field is not expected to have a noticeable effect on dose measurement.

Conclusions

While the presence of the magnetic field limited the choice of QA devices, it was found that satisfactory methods for MRI-IMRT machine QA exist and can be successfully employed. Drs. Green, Goddu, and Mutic served as scientific consultants for ViewRay, Inc. Dr. Mutic is on the clinical focus group for ViewRay, Inc., and his spouse holds shares in ViewRay, Inc.

Observation of Radiation-induced Tissue Signal Intensity Changes With the First Commercial MRI-guided IMRT System

Green, O., Hu, Y., Noel, C., Olsen, J. & Mutic, S. (2012). Observation of Radiation-induced Tissue Signal Intensity Changes With the First Commercial MRI-guided IMRT System. *International Journal of Radiation OncologyBiologyPhysics*, 84, S758-759.

http://www.redjournal.org/article/S0360-3016(12)02973-2/fulltext

Article Outline

- Purpose/Objective(s)
- Materials/Methods
- Results
- Conclusion
- Copyright

Purpose/Objective(s)

To describe radiation-induced tissue signal intensity changes observable with a commercial MRI-Guided IMRT system and the potential utility of these images. The MRI-Guided IMRT system was recently installed at our institution. The stand-alone system is comprised of a 0.35-T double-doughnut MRI and a gantry housing three Co-60 sources that provide IMRT delivery with 600 cGy maximum dose rate at isocenter. Prior to installation of the sources, a patient imaging study was conducted to evaluate the imaging quality of this hybrid system. During the course of this imaging study, an observation was made of radiation-induced signal intensity change in the liver of a patient who had recently completed radiation therapy for pancreatic cancer. Previously published reports noted tissue changes visible on CT and 1.5-T diagnostic MRI systems; this is the first observation of radiation-induced tissue change with a low-strength MRI specifically designed for integration with a radiation delivery system.

Materials/Methods

The patient's radiation prescription was 5500 cGy in 25 fractions delivered via 6-MV IMRT; the scan was performed ten days after completion of therapy. The PTV was located slightly left of mid-plane at the level of the liver; the signal intensity change was observed in the liver tissue. The visible stripe of affected tissue in the liver matches the path of one of seven roughly equally-spaced beams; the beam's relative weight was 20.2%. The total liver volume was 1476 cc, the volume of the tissue with visible change was contoured and determined to be approximately 160 cc.

Results

The dose received by the liver was well within accepted guidelines: the volume receiving 3000 cGy was less than 4% (50 cc). Total liver mean dose was 614 cGy, with a maximum of 5651 cGy where the PTV contour overlapped with the liver. The mean dose to the area of visible signal intensity change was 1498 cGy. Previously published reports of hepatic injury do not include cases of such low dose; the tissue changes visible with CT were due to 5000 cGy and above directly to the liver.

Conclusion

In addition to hepatic changes, it has been previously reported that radiation-induced changes appear in head-and-neck tissues, as well. The MRI-Guided IMRT system enables daily imaging and may in turn facilitate correlations between clinical data and visible tissue changes throughout and after therapy.

Realizing the QUANTEC Vision by Applying Weighted Hybrid Iterative Spiral K-Space Encoding Estimation (WHISKEE) to Actual Dose (D_A) Accumulation via Image Deformation (D_AA_VID)

Green, O., Hu, Y., Zeng, Q., Nana, R., Patrick, J., Shvartsman, S., Eagan, T., Mutic, S., & Dempsey, J. (2012). Realizing the QUANTEC Vision by Applying Weighted Hybrid Iterative Spiral K-Space Encoding Estimation (WHISKEE) to Actual Dose (D_A) Accumulation via Image Deformation (D_AA_VID). *International Journal of Radiation OncologyBiologyPhysics,* 84, S758-759.

http://www.redjournal.org/article/S0360-3016(13)00712-8/fulltext

Article Outline

- Purpose/Objective(s)
- Materials/Methods
- Results
- Conclusions
- Copyright

Purpose/Objective(s)

As quoted in the vision paper of QUANTEC: "Accurately estimating (true dose) DA is a critical element in the drive to maximize the performance and safe application of radiation therapy for the patient." We present here a novel compressed-sensing algorithm with spiral K-space data acquisition and a process to acquire high frame rate volumetric MR images of a sufficient quality to support actual dose (DA) accumulation via image deformation (DAAvID).

Materials/Methods

A commercially-available MRI-IGRT system was used for this investigation. Currently, the system allows real-time planar (2D) imaging at four frames per second. To achieve high-quality, low-noise volumetric images during radiation therapy delivery, an investigation of a novel compressed-sensing algorithm is proposed. This method employs weighted hybrid iterative spiral K-space encoding estimation (WHISKEE) to enable fast, high quality volumetric imaging at up to four frames per second. Deformable image registration will subsequently be used to quantify the effects of motion and deformation, and determine the actual distribution of dose accumulated in both normal tissues as well as in target volumes using the integrated Monte Carlo dose calculation. This, in turn, will enable the quantification of the effects of geographic misses on target volume and critical structure doses.

Results

A prototype model of the technique was implemented on the pre-clinical ViewRay system to obtain images of a volunteer human pelvis at a rate of 1 volume per second (VPS). Each volume was acquired in 936 ms, and consisted of 30 axial frames. The field of view was 38×38×11.2 cm. The reconstruction rate for the usual 2D images on ViewRay is 10 frames per second on a single CPU core; the volumetric images taken at 1 VPS were reconstructed 1.6 times slower with the existing system. A 64-core computer cluster system can enable reconstruction at 4 volumes per second.

Conclusions

Overview of the complete method as well as up-to-date results of the implementation and validation, now on-going, will be presented.

Evaluation of Surface, Peripheral, and Buildup Dose in MR-IGRT

Green, O., Wooten, H., Hu, Y., Santanam, L., Li, H. & Mutic, S. (2013). SU-ET-139: Evaluation of Surface, Peripheral, and Buildup Dose in MR-IGRT. *Medical Physics*, 40(6), 236.

http://dx.doi.org/10.1118/1.4814574

Purpose

To determine the effect of the magnetic field on surface and buildup dose in radiotherapy using MR-IGRT, specifically measured with a Co-60 system.

Methods

A commercially-available MR-IGRT system was used to measure surface, peripheral, and build-up dose due to thermoplastic head immobilization masks. Both radiographic (Kodak EDR2) and radiochromic (EBT2) film types were used for surface measurements. A small-volume ionization chamber was used for peripheral dose measurements. Several types of thermoplastic masks from three different manufacturers were chosen; radiochromic film was used to measure possible dose to skin under the masks. Comparisons were made using these masks with 6-MV photon beams delivered by a Varian Truebeam machine.

Results

For a 10×10 cm field size at 100 SSD, the surface dose as normalized to maximum dose (at 0.5 cm) was determined to be about 30% as measured by both EDR and EBT2 films. Peripheral dose with an open 10x10 field at 10 cm depth matched previously published data for Co-60. Skin dose due to thermoplastic mask buildup was at least 30% higher (depending on mask construction) with Co-60 as compared to 6-MV due to its lower energy.

Conclusion

While the magnetic field of an integrated MR-IGRT system is expected to reduce skin dose by sweeping away contamination electrons, the use of Co-60 introduces the added challenge of carefully choosing immobilization devices in order to preserve the skin-sparing effect of the MR. Drs. Green, Hu, and Mutic have served as consultants to ViewRay, Inc.

TG-51 Calibration of First Commercial MRI-Guided IMRT System in the Presence of 0.35 Tesla Magnetic Field

Goddu, S., Green, O., & Mutic, S. (2012). WE-G-BRB-08: TG-51 Calibration of First Commercial MRI-Guided IMRT System in the Presence of 0.35 Tesla Magnetic Field. *Medical Physics*, 39(6), 3968.

http://dx.doi.org/10.1118/1.4736194

Purpose

The first real-time-MRI-guided radiotherapy system has been installed in a clinic and it is being evaluated. Presence of magnetic field (MF) during radiation output calibration may have implications on ionization measurements and there is a possibility that standard calibration protocols may not be suitable for dose measurements for such devices. In this study, we evaluated whether a standard calibration protocol (AAPM- TG-51) is appropriate for absolute dose measurement in presence of MF.

Methods

Treatment delivery of the ViewRay (VR) system is via three 15,000Ci Cobalt-60 heads positioned 120-degrees apart and all calibration measurements were done in the presence of 0.35T MF. Two ADCL- calibrated ionization-chambers (Exradin A12, A16) were used for TG-51 calibration. Chambers were positioned at 5-cm depth, (SSD=105cm: VR's isocenter), and the MLC leaves were shaped to a 10.5cm × 10.5 cm field size. Percent-depth-dose (PDD) measurements were performed for 5 and 10 cm depths. Individual output of each head was measured using the AAPM- TG51 protocol. Calibration accuracy for each head was subsequently verified by Radiological Physics Center (RPC) TLD measurements.

Results

Measured ion-recombination (Pion) and polarity (Ppol) correction factors were less-than 1.002 and 1.006, respectively. Measured PDDs agreed with BJR-25 within ±0.2%. Maximum dose rates for the reference field size at VR's isocenter for heads 1, 2 and 3 were 1.445±0.005, 1.446±0.107, 1.431±0.006 Gy/minute, respectively. Our calibrations agreed with RPC- TLD measurements within ±1.3%, ±2.6% and ±2.0% for treatment-heads 1, 2 and 3, respectively. At the time of calibration, mean activity of the Co-60 sources was 10,800Ci±0.1%.

Conclusions

This study shows that the TG- 51 calibration is feasible in the presence of 0.35T MF and the measurement agreement is within the range of results obtainable for conventional treatment machines. Drs. Green, Goddu, and Mutic served as scientific consultants for ViewRay, Inc. Dr. Mutic is on the clinical focus group for ViewRay, Inc., and his spouse holds shares in ViewRay, Inc.

Automatic Deformable Registration on Prostate Cine-MRI Images for Studying Intra-fraction Motion in Supine and Prone Position with and without Rectal Balloon

Hsi, W., Vargas, C., Saito, A., Dempsey, J., Keole, S., Lin, L., et al. (2008). Automatic Deformable Registration On Prostate Cine-MRI Images For Studying Intra-fraction Motion In Supine And Prone Position With And Without Rectal Balloon. *International Journal of Radiation OncologyBiologyPhysics*, 72(1), S557-S557.

http://www.redjournal.org/article/S0360-3016(08)02088-9/fulltext

Article Outline

- Purpose/Objective(s)
- Materials/Methods
- Results
- Conclusions
- Copyright

Purpose/Objective(s)

Prior studies of intra-fraction motion had relied on points to define prostate position. They include X-ray, Calypso electromagnetic markers or point of interests (POIs) in cine-MRI images. Defining the prostate position by points provide a surrogate for the prostate position. We present the first volume analysis of prostate the intra-fraction motion for patients at different settings with or without a rectal balloon (WRB) and without (WORB).

Materials/Methods

A total of 68 Cine-MRI studies were done in 17 different series with 4 scans per series, consisting of supine and prone, each WRB and WORB. Each san was performed for 4 minutes; the time is close to complete one field of proton treatment. Furthermore, it is the maximum time before the chemical shift to distort the spatial resolution of images due to the short excitation time between pulses (240 ms). By employing automatic deformable registration developed by ViewRay Inc., the prostate and pelvis structures were segmented. The accuracy of automatic segmentation was carefully inspected. A program was then developed to obtain centroid of prostate from the prostate outline. Prostate position of each image was evaluated in reference to the initial image.

Results

After inspecting automatic segmentation, no correction was needed for prostate outline. The mean prostate position over 240 seconds of all series was small: supine WRB 0.217 mm, WORB 0.397 mm and prone WRB 0.267 mm, WORB 0.318 mm, although smaller for the supine patients WRB ($p < 0.0001$). However, the variation of the prostate position during 240s was larger: supine WRB 1.01 mm, WORB 1.20 mm and prone WRB 1.47 mm, WORB 2.144 mm ($p < 0.001$). The margins needed to cover all patients 100% of the treatments during 95% of the single beam time (4 min) were: supine WRB 2.21 mm, WORB 2.75 mm and prone WRB 3.13 mm, WORB 4.53 mm ($p < 0.001$). A strong relation was seen between time and prostate motion: the prostate will remain within 2.0 mm and 3.2 min, respectively, in 2 and 4 minutes for the best case, supine WRB, and within 4.2 mm and 5.3 mm for the worse case, prone WORB. The probabilities for prostate staying within +/– 1 mm to its initial position are: 94% supine WRB x-axis (i.e., anterior-posterior) and 88% y-axis (i.e., superior-inferior); supine WORB 78% x-axis and 75% for y-axis; prone WORB 67% x-axis and 78% axis; and prone WORB 55% x-axis and 83% y-axis.

Conclusions

After employing the image guidance (either cone-beam or X-rays) to setup patient, intra-fraction motion becomes the largest error and needs to be included into the treatment margin. Reducing the time between after setup and the finalization of treatment or beam will require smaller intra-fraction margin. Prostate position for supine WRB Cine-MRI scans was very stable and can use a small treatment margin.

Image Performance Characterization of an MRI-Guided Radiation Therapy System

Hu, Y., Green, O., Feng, Y., Du, D., Wooten, O., Li, H. , Santanam, L., Parikh, P., Olsen, J., & Mutic, S. (2013). Image Performance Characterization of an MRI-Guided Radiation Therapy System. *International Journal of Radiation OncologyBiologyPhysics*, 87, S13.

http://www.redjournal.org/article/S0360-3016(13)00710-4/fulltext

Article Outline

- Purpose/Objective(s)
- Materials/Methods
- Results
- Conclusions
- Copyright

Purpose/Objective(s)

We assessed image performance of the first commercial MRI-guided radiation therapy system. The on-board imaging unit for the system is a 0.35 Tesla MRI scanner. The goal of this study was to characterize the performance of this on-board imaging unit.

Materials/Methods

We evaluated the image performance of an MRI-guided radiation therapy system. The spatial integrity test was performed using an in-house developed 3D rectangular geometric accuracy phantom. Both MRI and CT images of the phantom were acquired. Control point locations determined using MR images were compared to those determined using CT images to evaluate geometric distortion. The ACR phantom tests were performed based on the procedures documented in the ACR manual. The SNR and uniformity tests were performed according to NEMA Standards MS 1-2008, MS 3-2008, MS 6-2008 and MS 9-2008. The acoustic noise was measured according to NEMA standards MS 4-2010. The RF calibration and RF phase stability tests were performed according to procedures recommended by AAPM report No. 34.

Results

The geometric distortion for all control points was less than 1 mm within the DSV (diameter of spherical volume) of 200 mm and less than 2 mm within the DSV of 350 mm. For planning images, typical geometric distortion was approximately 0.2 mm and 0.6 mm for DSV of 200 mm and 350 mm, respectively. For tracking images, typical geometric distortion was around 0.1 mm for both DSV of 200 mm and 350 mm. All ACR phantom imaging tests passed. More specifically, the average deviation from the prescribed slice thickness was 0.62 mm, the average deviation from the prescribed slice position was 1.64 mm, high contrast spatial resolution was 0.9 mm, and the low contrast detectability test resolved 19 spokes for T2 weighted images and 13 spokes for T1 weighted images. In SNR and uniformity test, the maximum absolute SNR deviation from the mean of all SNR values was 1.62%, 6.98% and 7.22% for the body coil, combined torso coil and combined head/neck coil, respectively, which were all within the specification. In the acoustic noise test, the noise of the loudest sequence at the loudest spot inside the patient bore was 120.2 dB (average) and 123.6 dB (peak). Therefore, hearing protectors are required to bring the noise level down to 99 dB. In the RF (radiofrequency) calibration test, the plot of the signal intensity versus flip angle shows a sinusoidal pattern with the highest signal occurring at the 90° flip angle. In the RF phase stability test, time that FID (free induction decay) first crosses the time axis had a stability of less than 2% for both real and imaginary channels.

Conclusions

The on-board 0.35 Tesla MRI imaging system exhibits satisfactory performance that meets well-established national recommendations.

Initial Experience with the ViewRay System - Quality Assurance Testing of the Imaging Component

Hu, Y., Green, O., Parikh, P., Olsen, J., & Mutic, S. (2012). TH-E-BRA-07: Initial Experience with the ViewRay System-Quality Assurance Testing of the Imaging Component. *Medical Physics,* 39(6), 4013.

http://www.aapm.org/meetings/2012AM/PRAbs.asp?mid=68&aid=19067

Purpose

The ViewRay system is a MRI-guided radiotherapy system. The first commercial ViewRay system (pending 510(k) clearance) is under installation at our institution. In this work, we present initial quality assurance testing of the 0.35T MR imaging component of the ViewRay system.

Methods

Quality assurance testing was performed on an ACR phantom following ACR recommendations. All testing was performed prior to installation of the 60Co sources. The phantom was placed at the isocenter of the MRI scanner. Sagittal localizer, axial T1 and T2 weighted scans were acquired. For all 3 scans, FOV was 250mmx250mm and the acquisition matrix was 256x256. TR and TE were 200ms and 20ms for the localizer, 500ms and 20ms for the T1 scan, and 2000ms and 20ms(80ms) for the T2 scan. The Localizer and T1 scan used spin echo acquisition and the T2 scan used double spin echo acquisition. 25 averages were used for T1 acquisition and 9 averages were used for T2 acquisition. The T1 scan was repeated with the prescan normalization option turned off to estimate the percent ghosting. Seven tests were performed including geometric accuracy, spatial resolution, slice thickness, slice position accuracy, image intensity uniformity, percent ghosting and low contrast detectability.

Results

All tests passed the ACR recommended criteria. The results and specifications (in parentheses) are listed below. Geometric accuracy was 148.6mm (148mm±2mm) and 190.2mm (190mm±2mm). Spatial resolution was 0.9mm (‹1.0mm). Slice thickness was 5.4mm (5.0mm±0.7mm). Slice position accuracy was 3.1mm, 0.0mm, 3.0mm and 0.0mm (±5mm). Image intensity uniformity was 93% and 92% (›87.5%). Percent ghosting was 0.0016 (‹0.025). Low contrast detectability was 10 and 13 (=9).

Conclusions

Although the ViewRay system is not designed for diagnostic purposes, our initial experience with its imaging component showed promising results. Quality assurance testing will be repeated following installation of the 60Co to confirm imaging performance.

MRI-Guided Radiation Therapy

Jaffray, D., Mutic, S., Fallone, B., & Raaymakers, B. (2013). MO-A-WAB-01: MRI-Guided Radiation Therapy. *Medical Physics*, 40(6), 390.

http://dx.doi.org/10.1118/1.4815216

The concept of integrating a magnetic resonance imaging (MRI) scanner with a therapy radiation source, either a therapy linear accelerator (linac) or 60 Co, emerged as a feasible novel approach for MRI-guided radiation therapy (i.e. MRIgRT or MRgRT) in recent years. The main motivation for the technological development of such radiotherapy systems is to provide state of the art MR imaging inside the treatment room to guide the treatment delivery. MRI offers the capability to visualize soft-tissue as well as to perform physiological assessment of healthy and tumor tissues. The aim of MRIgRT is to facilitate adaptive radiotherapy by using on demand MRI data to update and personalize patient treatments.The MRI-linac/ 60 Co system integration is a challenging task due to the intrinsic default incompatibility between the sub-components. Multiple interdependent issues need to be resolved in order to achieve the optimal operation of the MRI scanner and the radiation source(s) such as: a) radiofrequency (RF) interference, b) magnetic field coupling, c) perturbation of the dose deposited in tissue due to the presence of an external magnetic field, and d) escalation of patient skin dose. This translates into solving a complex optimization problem which drives the overall system architecture. The session will provide an overview of the MRI-guided radiation therapy systems. The speakers will present the specifics of their proposed designs and the latest technological developments (hardware and software). They will also discuss key aspects related to the clinical implementation of their systems such as safety, applications, workflows, quality control, staffing models for supporting the infrastructure, and preliminary data.

Learning Objectives:

1) Understand the main concepts of MRI-guided radiation therapy;
2) Understand the issues and proposed solutions related to the integration of MRI-guided radiotherapy systems;
3) Understand the advantages and limitations of MRI-guided radiotherapy systems.

First Commercial Hybrid MRI-IMRT System

Mutic S. (2012). WE-A-BRA-02: First Commercial Hybrid MRI-IMRT System. *Medical Physics*, 39(6), 3934.

http://www.aapm.org/meetings/2012AM/PRAbs.asp?mid=68&aid=19832

The first commercially available MRI-guided IMRT (MRIGRT) system (ViewRay, Cleveland, OH) has been installed at Washington University in St. Louis. This novel medical instrument combines magnetic resonance imaging and intensity modulated radiation therapy at a single isocenter for simultaneous use during therapy along with automated tissue tracking and beam control based on images of soft tissue acquired in real time rates of 2-4 FPS simultaneous to the delivery. The purpose of this presentation is to describe and evaluate the technical aspects of the instrument as well as its adaptive and image guided radiotherapy workflows. The ViewRay system consists of a 0.35-T double-doughnut MRI coupled with a gantry that houses three radiotherapy heads containing 15,000-Ci Co-60 sources (120° apart). IMRT delivery is enabled by 3 doubly-focused MLCs that serve as the only collimators for each head, allowing a maximum field size of 27 cm2 at the 105-cm isocenter. MRI imaging is used prior to and during delivery for patient setup evaluation, adaptive radiotherapy, and tissue tracking and beam control based on real time 2-4 FPS imaging (2 FPS in 3 parallel planes or 4 FPS in a single plane). The fast MR imaging coupled with fast auto-contouring, image fusion that can transfer tissue densities (via contours through bulk density or from fused CT imaging), and dose calculation facilitate real time dose delivery evaluation, on couch reoptimization, and replanning when necessary. The instrument's multiframe per second MR imaging enables motion correlated delivery based on the actual target volumes rather than on surrogates. Following treatment, the image, contours, and control system data produce a record of the delivery that is automatically recorded and registered to the orginal plan for evaluation. All imaging and adaptive features are controlled by clinician directives at the planning stage and can be set as required, optional, or prohibited. The design and capabilities of the system create several novel concepts and promising capabilities in RT delivery from imaging and treatment to workflow and QA/QC. This presentation discusses the initial assessment of these features and their implementation and the early clinical experience with the system including validation of its capabilities.

Learning Objectives

1) To describe technical design and capabilites of ViewRay system
2) To describe adaptive and image guided RT workflow with this system
3) To present initial validation assessment of the system

Feasibility of Bowel Tracking Using Onboard Cine MRI for Gated Radiotherapy

Noel, C., Olsen, J., Green, O., Hu, Y. & Parikh, P. (2012). TU-G-217A-09: Feasibility of Bowel Tracking Using Onboard Cine MRI for Gated Radiotherapy. *Medical Physics*, 39(6), 3928.

http://dx.doi.org/10.1118/1.4736032

Purpose

Bowel toxicity can be difficult to manage in the treatment of abdominal cancers. The bowel experiences large motion during treatment, causing it to enter high-dose regions. Real-time MR imaging during radiotherapy allows for potential visualization and dosimetric avoidance of the bowel during treatment. To investigate the feasibility of real-time 'bowel-gated' treatment using onboard MRI, we assessed two bowel-tracking algorithms on 32 cine imagesets acquired with the ViewRay hybrid MR- radiotherapy unit.

Methods

The Viewray(TM) System, which is an integrated 0.35T MR-Co-60 system that is pending 510k approval, was used to acquire 32 cine image sets in 5 patients under an IRB-approved trial. Each imageset was acquired in 2D (coronal or sagittal orientation) for an average duration of 0.5-2.5 minutes at a frame rate of 4 frames/s. The initial position of the bowel was manually contoured on the first image frame. Two algorithms were evaluated in tracking bowel from its initial position throughout its motion for the duration of the cine set - a normalized cross- correlation (NCC) algorithm, and a weighted NCC (WNCC) algorithm. To assess the tracking feasibility and accuracy of these two methods, the initial contour was virtually shifted with the tracked motion and displayed on tracked cine images. The agreement between the shifted contour and the border of the bowel was manually inspected and noted for each frame.

Results

Both algorithms successfully tracked 31/32 cases in 100% of frames. The WNCC algorithm outperformed the NCC algorithm in speed, with a mean processing speed of .007s versus .013s, respectively, and captured a greater range of motion in all cases.

Conclusions

The demonstrated feasibility of bowel tracking on cine MR imagesets indicates its potential successful use in real-time bowel tracking and gated radiotherapy. While both algorithms performed well, the WNCC algorithm was superior in processing speed and sensitivity to bowel motion.

Feasibility of Single and Multiplane Cine MR for Monitoring Tumor Volumes and Organs-at-Risk (OARs) Position During Radiation Therapy

Olsen, J., Noel, C., Spencer, C., Green, O., Hu, Y., Mutic, S., & Parikh, P. (2012). Feasibility of Single and Multiplane Cine MR for Monitoring Tumor Volumes and Organs-at-Risk (OARs) Position During Radiation Therapy. *International Journal of Radiation OncologyBiologyPhysics*, 84, S742.

http://www.redjournal.org/article/S0360-3016(12)02929-X/fulltext

Article Outline

- Purpose/Objective(s)
- Materials/Methods
- Results
- Conclusions
- Copyright

Purpose/Objective(s)

Multiple groups are working on integrating MR guidance during radiation therapy. A systematic evaluation of images is required to identify targets and OARs that may be tracked or intervened on. The feasibility of target and OAR visualization with cine MR acquired using an integrated MR-Co-60 system was evaluated in this study.

Materials/Methods

Nineteen patients undergoing radiation therapy were enrolled on an IRB approved protocol, and underwent MR imaging on the 0.3T MR-Co-60 system. 35 cine image sets were acquired in the transverse (n = 10), sagittal (n = 18), or coronal (n = 7) plane with a slice thickness of 5 (n = 27) or 7 (n = 8) mm. The acquisition rate was 4 frames per second (fps) for images acquired in a single plane (n = 18), and 2 fps for images acquired simultaneously in 3 parallel planes (n = 17). OAR were selected from a published naming taxonomy. All radiation therapy targets and OARs that were within the imaging field of view for each dataset were evaluated by 3 radiation oncologists (JRO, PJP, CRS) to study the feasibility of monitoring anatomical motion. Physicians were specifically asked if image quality would permit manual visualization of the target or OAR for the purpose of gated radiation therapy.

Results

Physicians evaluated 21 total target structures, and 321 total OAR structures in 35 image sets, including 13 unique targets and 58 unique OARs that were within the field of view. 7/13 targets were identified with consensus agreement by all 3 physicians that image quality was suitable for manual gating. Radiation therapy targets that were well visualized included tumors of the cervix, liver, lung, nasopharynx, and the breast lumpectomy cavity. 44/58 OARs were identified with consensus agreement by all physicians that image quality was suitable for manual gating. Well visualized OARs included the aorta, atrium, base of tongue, bladder, brainstem, breast, bronchial tree, carina, cerebellum, cerebrum, colon, duodenum, esophagus, femur, heart ventricle, kidney, larynx, liver, lung, mainstem bronchus, masseter muscle, optic nerve, pelvic bones, pelvic vessels, penile bulb, penis, pericardium, pharyngeal constrictors, pituitary, prostate, pulmonary vessels, rectum, retina (globe), rib, sacrum, seminal vesicles, small bowel, spinal cord, spleen, stomach, subclavian vessels, tongue, trachea, uterus, and vertebral body. A unanimous consensus was reached for 19/21 (90%) of targets and 308/321 (96%) of critical structures evaluated.

Conclusions

A wide variety of radiation therapy targets and OARs were well visualized on single and multi-plane cine 0.3T MRI. Future work including testing automated tracking algorithms and developing clinical trials for the visualized targets and OARs is needed to fully exploit MRI-guided radiation therapy.

Comparison of Onboard Low-field MRI Versus CBCT/MVCT for Anatomy Identification in Radiation Therapy

Parikh, P., Noel, C., Spencer, C., Green, O., Hu, Y., Mutic, S., & Olsen, J. (2012). Comparison of Onboard Low-field MRI Versus CBCT/MVCT for Anatomy Identification in Radiation Therapy. *International Journal of Radiation OncologyBiologyPhysics*, 84, S133.

http://www.redjournal.org/article/S0360-3016(12)01088-7/fulltext

Article Outline

- Purpose/Objective(s)
- Materials/Methods
- Results
- Conclusions
- Copyright

Purpose/Objective(s)

Multiple groups are investigating MR-XRT devices, but are using different field strength MR. Moreover, a comparison of MR versus available onboard imaging (CBCT/MVCT) has not been performed. We compared visualization of patient anatomy on images acquired on a 0.35T MR-Co-60 system to those acquired with CBCT/MVCT.

Materials/Methods

Fourteen patients undergoing image guided radiation therapy for cancer in the abdomen (n = 3), head/neck (n = 3), thorax (n = 2), and pelvis (n = 6) were enrolled on an IRB approved protocol and imaged with a 0.35T onboard MRI. Sequences varied depending on the site. CBCT/MVCT image sets used for routine treatment localization were collected for each patient within 2 weeks of MRI imaging. For each of the 14 patients, the volumetric MRI and CBCT/MVCT image sets were displayed side-by-side on clinical image viewing software and independently reviewed by three radiation oncologists (PJP, JRO, and CRS). Each physician was asked to evaluate which image set (if either) offered better visualization of the target and individual organs at risk (OAR), as derived from a standardized list of site-specific critical structures (Santanam, IJROBP, 2012).

Results

Fifteen to 24 OARs were evaluated per anatomical site (n = 15 for the abdomen, n = 24 for the head/neck, thorax, and pelvis). In total, 234 OARs and 10 unique target structures were compared for visualization on MRI and CBCT/MVCT image sets by each physician. At least 2/3 physicians evaluated MRI as offering better visualization for 71% of structures, CBCT offering better visualization in 9% of structures, and both offering equivalent visualization in 19% of structures. Physicians agreed unanimously in consensus for 74% and in majority for 99% of structures evaluated, respectively. For 1% of structures, no consensus was reached. For structures that were better visualized on MRI, 100% of the time included the anal canal, bladder, blood vessels, brachial plexus, lobes of the brain, brain stem, cerebellum, colon, cranial nerves, duodenum, esophagus, most structures of the heart, hippocampus, kidneys, liver, optic chiasm, optic nerve, parotids, penile bulb, pituitary gland, prostate, rectum, seminal vesicles, small bowel, spleen, stomach, submandibular glands, spinal cord, uterus, and vagina. Targets were better visualized on MRI in 4/10 cases, and were never better visualized on CBCT/MVCT images.

Conclusions

Low field MR provides better anatomic verification of many radiation therapy targets and most organs at risk as compared to CBCT/MVCT. Further work is needed to quantify improvements for specific tasks, such as repositioning and adaptive planning.

A Comparison of IMRT Plans for the ViewRay MR-Guided RT System with TomoTherapy and Pinnacle

Saenz, D., Bayouth J., & Paliwal B. (2013). SU-E-T-614: A Comparison of IMRT Plans for the ViewRay MR-Guided RT System with TomoTherapy and Pinnacle. *Medical Physics*, 40(6), 347.

http://www.aapm.org/meetings/2013AM/PRAbs.asp?mid=77&aid=21124

Purpose

To begin to assess the treatment planning capabilities of the ViewRay MR-guided radiotherapy system.

Methods

Treatment plans created using ViewRay software were compared with previously completed Pinnacle and TomoTherapy plans from patients in our clinic. Sites such as pancreas were chosen due to the soft-tissue contrast which makes them candidates for MR-image guidance with ViewRay. CT images and structure sets were exported from their original planning systems and imported into ViewRay. MR images were not the focus of this investigation since we required a direct comparison with existing plans utilizing CT. ViewRay plans were created as equivalently as possible with the original planning environment, matching prescription and normal structure priorities. The resulting isodose lines were visually assessed for conformality. Dose-volume histograms were extracted from ViewRay and plotted together with those from the original planning system. Finally, ViewRay plans were also examined by their ability to meet QUANTEC dose restraints.

Results

A pancreas plan created using the images of a patient who underwent IMRT with TomoTherapy resulted in satisfactory conformality assessed by the coverage of the 98% isodose line. The DVH demonstrated shallower dose fall-off for the PTV compared with TomoTherapy, as expected for a Cobalt-60 based treatment. Normal tissue DVH lines for ViewRay surpassed QUANTEC dose constraints or performed as well as TomoTherapy for all structures except kidney. Comparison with non-IMRT Pinnacle cases also exhibited good conformality and satisfied QUANTEC restraints.

Conclusions

ViewRay created a feasible plan generally matching most normal tissue restrictions. Of course, the IMRT gold-standard TomoTherapy outperformed ViewRay regarding the steepness of DVH dose fall-off. In the future, more cases will be studied to perform a more complete analysis. Also, we will investigate the Co-60 dose profiles to assess penumbra directly. The ViewRay TPS has the potential for comparable plans in the hands of experienced planners.

Accurate Heterogeneous Dose Calculation for Lung Cancer Patients Without High Resolution CT Densities

Saito, A., Li, J., Liu, C., Olivier, K., & Dempsey, J. (2006). 2831Accurate Heterogeneous Dose Calculation For Lung Cancer Patients Without High Resolution CT Densities. *International Journal of Radiation OncologyBiologyPhysics*, 66(3), S677-S678.

http://www.redjournal.org/article/S0360-3016(06)02486-2/fulltext

Article Outline

- Purpose/Objective(s)
- Materials/Methods
- Results
- Conclusions
- Copyright

Purpose/Objective(s)

The aim of this study is to investigate the relative accuracy of megavoltage photon-beam dose calculations using bulk densities applied to 4 distinct regions identified as air, lung, soft tissue, and bone when compared to dose calculations performed with a full density CT. We are investigating the accuracy of this bulk density dose calculation technique for use in an on-board magnetic resonance imaging (MRI) image guided radiation therapy (IGRT) device that is under development at our institution. This IGRT device will utilize real-time MRI taken simultaneously to radiation delivery to compute the dose to the patient. Segmented MRI imaging studies can be used to identify bulk density regions in the patient, but the high resolution density information of CT imaging is lost with this technique. Our hypothesis is that bulk densities can provide an accurate method of heterogeneous photon-beam dose calculation, even in lung cancer patients.

Materials/Methods

To test our hypothesis, full CT resolution and bulk density treatment plans were generated for 17 lung cancer cases using a commercial treatment planning system with an adaptive convolution dose calculation algorithm (Pinnacle3, Philips Medicals Systems). Bulk densities were applied to regions identified by an isodensity segmentation tool for each case. Individual and population average densities were compared to the full resolution plan for each case. Monitor units were kept constant and no normalizations were employed. Dose volume histograms (DVH) and dose difference distributions were examined for all cases.

Results

The average densities as determined by CT number of the segmented air, lung, soft tissue and bone for the entire set of patients were 0.15, 0.32, 0.98 and 1.11 [g/cc], respectively. Minor density differences existed between the population averages and the individual cases. In all cases, the normal tissue DVH agreed to better than 1%. In 15 out of 17 cases, the target DVH agreed to better than 1%, while 2 cases with bullous emphysema showed inconsistent lung density and agreed to within 4%. Inclusion of pronounced lung vasculature and atelectasis as soft tissue was important for obtaining accurate results. Figure 1 shows the excellent agreement between the two methods: a) axial CT with 4 densities; b) Full CT; c) Overlay of DVHs; and d) axial dose difference.

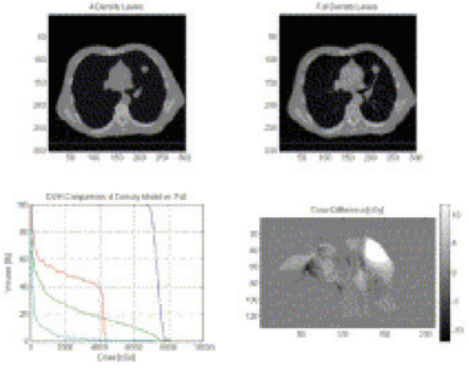

Conclusions

Dose calculation applying bulk tissue density to four regions provides an accurate method of heterogeneous dose calculation, which can be employed with MRI planning data. Dose calculation accuracy in cases with ehphysemic lung can be improved by assigning air to regions with bullous changes in the lung.

Monte Carlo Simulations of Air Cavities in Phantoms Submerged in Magnetic Fields

Yanez, R., & Dempsey, J. F. (2007). WE-C-AUD-04: Monte Carlo Simulations Of Air Cavities In Phantoms Submerged In Magnetic Fields. *Medical Physics*, 34(6), 2590.

http://dx.doi.org/10.1118/1.2761511

Purpose

We present studies in support of the development of a magnetic resonance imaging(MRI) guided intensity modulated radiation therapy(IMRT) device for the treatment of cancer patients. Fast and accurate computation of the absorbed ionizing radiation dose delivered in the presence of the MRImagnetic field are required for clinical implementation.

Method and Materials

The fast Monte Carlo simulation code DPM, optimized for radiotherapy treatment planning, is modified to simulate electron transport in uniform, static magnetic fields. Results: Simulations of dosedeposition in inhomogeneous phantoms in which a layer of air is sandwiched in water shows that a lower MRI field strength is to prefer in order to avoid dose build-up, due to returning electrons, in tissue surfaces. For a magnetic field of 0.3 T, cavities of up to several millimeters in thickness are safe from build-ups. Larger cavities require the use of opposing beams to cancel out the effect of returning electrons.

Conclusions

The effect of a B=0.3 T magnetic field in the dosedeposition by a Co-60 source is only appreciable in large air cavities, where a dose build-up due to returning electrons is formed near material boundaries. Cavities with dimensions smaller than the gyration radius are not severely affected by dose build-ups. For B=0.3 T cavities of the order of several millimeters are safe from dose build-ups. Research sponsored by ViewRay Incorporated.

Visibly Different

2 Thermo Fisher Way
Oakwood Village, OH 44146
+1 440 703 3210
www.viewray.com